Korean J. Chem. Eng., **26**(3), 902-906 (2009)

Methanol selective oxidation to dimethoxymethane on $H_3PMo_{12}O_{40}$/SBA-15 supported catalysts

Heqin Guo*,, Debao Li*, Haicheng Xiao*,**, Jianli Zhang*,**, Wenhuai Li*, and Yuhan Sun*,†**

*State Key Laboratory of Coal Conversion, Institute of Coal Chemistry, Chinese Academy of Sciences, Taiyuan, Shanxi 030001, P. R. China
**Graduate University of the Chinese Academy of Sciences, Beijing 100039, China
(*Received 31 July 2008 • accepted 24 November 2008*)

Abstract−A series of SBA-15 supported $H_3PMo_{12}O_{40}$ catalysts were prepared for the one-step oxidation of methanol to dimethoxymethane (DMM). The evaluation and characterization revealed that higher DMM selectivity obtained on the incipient wetness impregnation (IM) catalyst was related to the instability of $H_3PMo_{12}O_{40}$ on it. Raman spectra showed that 12-molybdophosphoric acid was more stable on the direct synthesis (DS) catalyst than on the IM catalyst and the existence of SBA-15 support enhanced the stability of $H_3PMo_{12}O_{40}$. Moreover, higher $H_3PMo_{12}O_{40}$ loading resulted in more acid sites and low DMM selectivity, furthermore the thermal pretreatment on $H_3PMo_{12}O_{40}$ influenced its structure and thus affected DMM selectivity.

Key words: 12-Molybdophosphoric Acid, SBA-15 Mesoporous Sieve, Methanol, Selective Oxidation, Dimethoxymethane

INTRODUCTION

Dimethoxymethane ($CH_3OCH_2OCH_3$, DMM), as an important chemical intermediate, is widely used as gasoline additive, building block in organic syntheses, and the precursor of the synthesis of concentrated formaldehyde streams and of polyoxymethylene dimethyl ethers useful as diesel fuel additives. Now, DMM is produced by the two-stage synthesis involving methanol oxidation to formaldehyde (HCHO) on silver or iron molybdate catalysts, followed by subsequent condensation reactions of methanol-formaldehyde mixtures using sulfuric acid or solid acid catalysts [1,2]. The complex process and higher cost inhibit DMM production and application. In contrast, the one-stage synthesis of DMM via partial oxidation of methanol, $3CH_3OH+1/2O_2 \rightarrow CH_3OCH_2OCH_3+2H_2O$, can avoid the drawbacks of the two-stage technique. Iwasawa et al. [3,4] have reported that ReO_x-based catalysts with high Re content (~10 wt%) selectively oxidized methanol to DMM with much higher rates and selectivities. But the high cost of ReO_x and its volatility at the required reaction temperatures (473-593 K) present significant hurdles to the application of it in the single-stage selective synthesis of dimethoxymethane.

It was agreed that two types of active sites were required for DMM formation, namely, the redox site and the acid site [5]. In this field, 12-molybdophosphoric acid has received much attention owing to its unique acid and redox activity [6-9]. However, the essential drawback of its low surface area and lower stability limits its application in catalytic reaction. As a potential support, SBA-15 has large pore diameter, thick pore wall and high hydrothermal stability [10]. In this paper, the SBA-15 supported 12-molybdophosphoric acid catalysts were prepared and applied to the one-step oxidation of methanol to DMM, furthermore the relationship of structure and performance for the direct oxidation of methanol to DMM was studied.

EXPERIMENTAL

1. Catalyst Synthesis

The SBA-15 was prepared by hydrothermal method described by Zhao et al. [11]. The IM catalysts were prepared by stirring SBA-15 and impregnation solution maintained at 323 K until the dryness evaporation. The catalysts were dried at 353 K overnight and calcined at different temperature for 5 h. The DS catalyst was prepared by adding 8.5 g TEOS to a mixture of 4.0 g P123 (triblock poly(ethylene oxide)-poly(propylene oxide)-poly(ethylene oxide) ($EO_{20}PO_{70}EO_{20}$)), 105 ml H_2O, 0.38 g 12-molybdophosphoric acid and 1.7 ml hydrochloric acid. The mixture was continuously stirred at 313 K for about 24 h and then transferred into Teflon-line autoclaves and heated at 373 K for 24 h. The obtained solid was filtered, dried and calcined in air for 5 h at 773 K.

2. Catalytic Performance Test

The catalytic oxidation reaction was carried out in a continuous flow fixed-bed reactor containing catalyst (1.5 g) diluted with ground quartz. The composition of the reagent was $Ar/O_2/CH_3OH=84.6/9.4/6.0$. The reaction products were analyzed by on-line gas chromatography (GC-950) using a propack T column and a TDX-01 column connected to TCD detector and FID detector, respectively. The products' selectivity was calculated on carbon molar base: $S_i = Y_i n_i / \Sigma Y_i n_i \times 100\%$, where i is the $CH_3OCH_2OCH_3$, CH_3OCH_3, HCHO, $HCOOCH_3$, CO_x, S_i the selectivity of product i, Y_i the number of carbon atoms of product i, and n_i is the molar of product i.

3. Catalysts Characterization

Surface areas of the catalysts were measured by a BET nitrogen adsorption method at 77.35 K using an ASAP 2000 machine, with the catalysts outgassed for 4 h at 483 K in vacuum (10.6 Torr) prior to measurement. XRD patterns were measured on a Bruker Advanced X-Ray Solutions/D8-Advance using Cu Kα radiation. The anode

†To whom correspondence should be addressed.
E-mail: yhsun@sxicc.ac.cn
‡This paper was presented at the 7th Korea-China Workshop on Clean Energy Technology held at Taiyuan, China, June 26-28, 2008.

was operated at 40 kV and 40 mA. The 2θ angles were scanned from 0.5° to 5°. FT-IR spectra were recorded on a Nicolet Magna 550 instrument with a DTGS KBr detector. Raman spectra were measured with a Renishaw-Uv-Vis Raman System 1000 Raman spectrometer (Kaiser Optical) and a frequency-doubled He: Cd laser at a wavelength of 325 nm. The Raman spectrometer was equipped with a CCD camera that was electrically cooled to 233 K in order to reduce thermal noise. Rotating-sample techniques were used to prevent the decomposition and/or reduction by the laser beam. Raman spectra were measured for DS and IM samples treated in flowing 20% O_2/He (O_2, Praxair, 99.999%; He, Air gas, 99.999%; 0.67 cm^3/s) at several temperatures for 3 h. The NH_3-TPD spectra were recorded in a fixed-bed reactor system equipped with a gas chromatograph. The catalyst (200 mg) was pretreated at 773 K under Ar flow (60 ml/min) for 2 h and then cooled to 323 K under Ar flow. Then NH_3 was introduced into the flow system. The TPD spectra were recorded at a temperature rising rate of 10 K/min from 323 to 900 K.

RESULT AND DISCUSSION

1. The Influence of Preparation Method

The XRD patterns of the DS and IM catalysts (with $PMo_{12}H$ loading of 13.2 wt%) are shown in Fig. 1. For these two catalysts, the hexagonal structure of SBA-15 was confirmed by a typical XRD patternconsisting of a strong peak (at 2θ around 0.8°) along with two weak peaks (at 2θ around 1.6° and 1.8°) [12,13]. While the peak intensity of the IM catalyst was weaker than that of the DS catalyst. This phenomenon could be explained as that the IM catalyst was prepared by impregnation method, $H_3PMo_{12}O_{40}$ might block the pore channel and weaken the long-range order of SBA-15. But for the DS catalyst, the $H_3PMo_{12}O_{40}$ was introduced into the liquid mixture during the synthesis process in which strong interaction between TEOS and $PMo_{12}H$ might occur. As a result, some of $H_3PMo_{12}O_{40}$ might incorporate into the pore wall without weakening the long-range order of SBA-15. This deduction was also verified by the textural properties of the catalysts as shown in Table 1. Compared with the IM catalyst, the DS catalyst had higher surface area, larger pore volume and pore size, which was an indication of the finely dispersed H_3 $PMo_{12}O_{40}$.

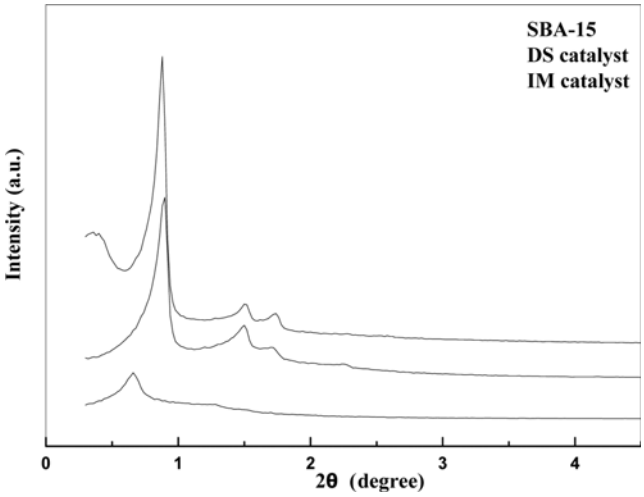

Fig. 1. The XRD patterns of the IM and DS catalysts.

Table 1. The textural properties of the catalysts

Catalysts	BET Surface are (m^2/g)	Pore size (nm)	Pore volume (cm^3/g)
SBA-15	747	7.14	1.26
DS catalyst	708	6.64	1.15
IM catalyst	655	6.58	1.05

The existing state of $H_3PMo_{12}O_{40}$ on SBA-15 was also studied by Raman spectra as shown in Fig. 2. The main characteristic features of the Keggin structure were observed at 1,012 cm^{-1}, 984 cm^{-1} and 836 cm^{-1}. The bands at 1,012 cm^{-1} and 984 cm^{-1} were assigned to terminal Mo=O stretching vibrations and the band around 836 cm^{-1} was assigned to bridging Mo-O-Mo (or P) stretching modes in the intact Keggin structure [5,15]. For the IM catalyst, the band at 1,012 cm^{-1} and 984 cm^{-1} remained almost unchanged, while a new band at 820 cm^{-1} corresponding to the characteristic peak of β-MoO_3 appeared, indicating that the Keggin structure was partly decomposed into β-MoO_3. However, For the DS catalyst, the characteristic peaks of $H_3PMo_{12}O_{40}$ were always observed, indicating that there might be some chemical interaction between $H_3PMo_{12}O_{40}$ and SBA-15 and thus inhibiting the decomposition of $H_3PMo_{12}O_{40}$.

The catalytic performance of methanol oxidation for DMM synthesis at 453 K is shown in Table 2. Compared with the different

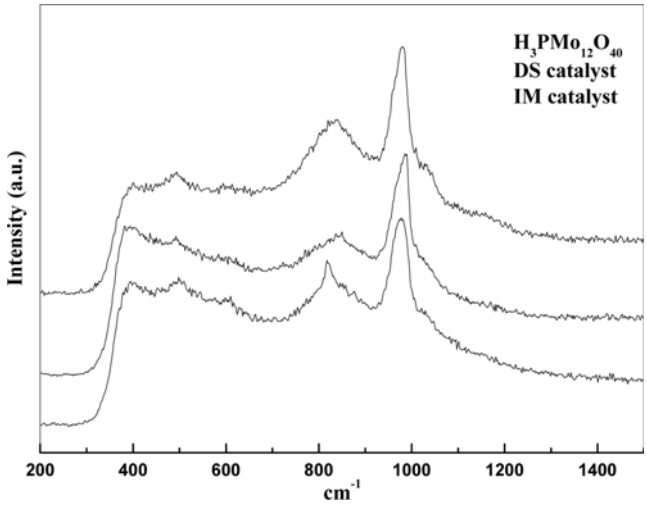

Fig. 2. The Raman spectra of the IM and DS catalysts.

Table 2. The effect of preparation methods on methanol oxidation

Catalysts	Methanol conv. (%)	Selectivity (%)				
		HCHO	DME	MF	DMM	COx
DS	22.19	18.26	38.67	17.25	24.83	0.99
IM	20.69	22.65	20.91	21.97	34.01	0.69

$H_3PMo_{12}O_{40}$/SBA-15 (13.2 wt%) pretreated at 773 K, CH_3OH/O_2/Ar=6.0/9.4/84.6, 453 K, 4,000 ml·g_{cat}·h^{-1}. DMM: Dimethoxymethane, HCHO: formaldehyde, MF: methyl formate, DME: dimethyl ether, COx: CO_2 (or CO)

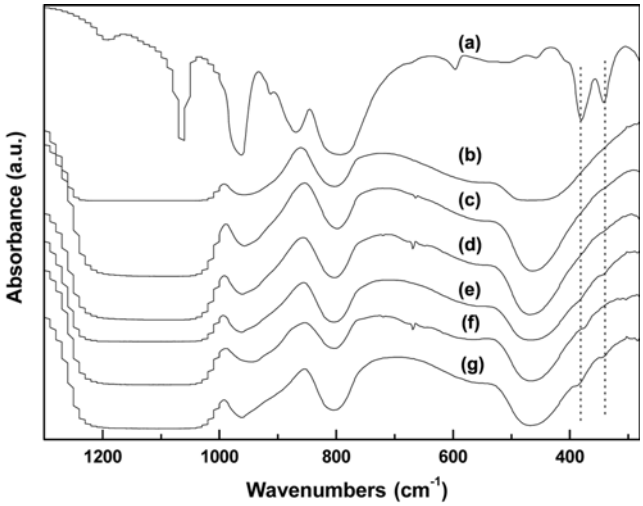

Fig. 3. The FT-IR spectra of the IM catalysts with different $H_3PMo_{12}O_{40}$ loading: (a) $H_3PMo_{12}O_{40}$, (b) SBA-15, (c) 9.1 wt%, (d) 13.2 wt%, (e) 16.6 wt%, (f) 20.9 wt%, (g) 28.5 wt%.

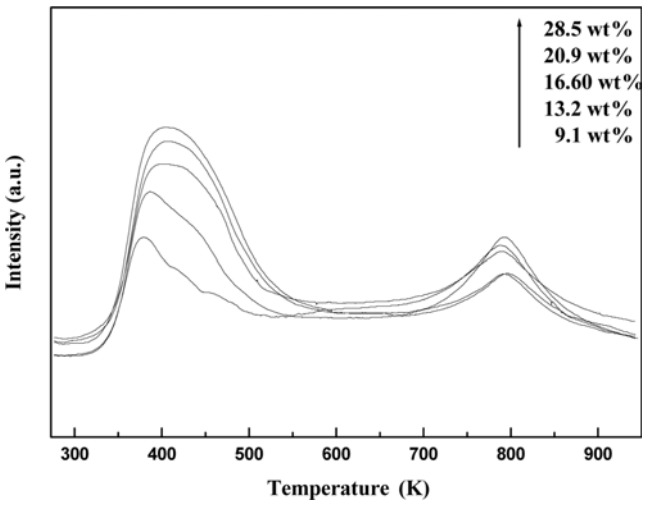

Fig. 4. The NH_3-TPD profiles of IM catalysts with different $H_3PMo_{12}O_{40}$ loading.

preparation methods, the IM catalyst achieved higher DMM selectivity. This could be explained as follows: (1) The differences of the dispersion degree of $H_3PMo_{12}O_{40}$ on SBA-15; (2) The differences of the existing state of $H_3PMo_{12}O_{40}$ on SBA-15. The first argument could be verified by the XRD patterns and the BET surface area of the catalysts as discussed above. The finely dispersed $H_3PMo_{12}O_{40}$ on the DS catalyst with high surface area might obtain much more acid sites preferring Dimethyl ether (DME) synthesis and thus resulted in lower DMM selectivity. The latter deduction was verified by Raman spectra of the catalysts. Compared with the DS catalyst, the partly decomposed $H_3PMo_{12}O_{40}$ on the IM catalyst could provide proper acid sites suit for DMM synthesis [5,14,15].

2. The Influence of $H_3PMo_{12}O_{40}$ Loading

In order to study the effect of $H_3PMo_{12}O_{40}$ loading on methanol oxidation reaction, a series of $H_3PMo_{12}O_{40}$/SBA-15 (IM) catalysts with different $H_3PMo_{12}O_{40}$ content were prepared and tested.

The FT-IR spectra of the IM catalysts are shown in Fig. 3. SBA-15 exhibited four main peaks at 1,100 cm^{-1}, 965 cm^{-1}, 800 cm^{-1}, 464 cm^{-1}, respectively. The typical peaks for $H_3PMo_{12}O_{40}$ observed at 1,066 cm^{-1}, 962 cm^{-1}, 873 cm^{-1}, 796 cm^{-1}, 381 cm^{-1}, 338 cm^{-1} were assigned to stretching vibration of ν_{as}P-O_d, ν_{ass}Mo-O_t, ν_{as}Mo-O_b-Mo, ν_{as}Mo-Oν_{as}-Mo and two low-frequency bands characteristic of the α-form of the $H_3PMo_{12}O_{40}$ anion, respectively [16]. The peaks at 1,066 cm^{-1}, 962 cm^{-1}, 873 cm^{-1} and 796 cm^{-1} were overshadowed by the strong framework vibration bands of SBA-15. Consequently, the characteristic peaks of $H_3PMo_{12}O_{40}$ were characterized by the two low-frequency bands of the α-form of the PMo_{12} anion. As $H_3PMo_{12}O_{40}$ loading below 20.9 wt%, these peaks could not be observed, which meant that $H_3PMo_{12}O_{40}$ was finely dispersed and the hexagonal structure of SBA-15 was well remained. And while $H_3PMo_{12}O_{40}$ loading exceeded 20.9 wt%, the peaks at 381 cm^{-1}, 338 cm^{-1} were observed, showing the appearance of bulk $H_3PMo_{12}O_{40}$.

The acidity of the catalysts was also studied by NH_3-TPD as shown in Fig. 4. Two types of acid centers, an intense peak with a maximum at about 410 K corresponding to the weaker acid site, and a wide much less intense peak at about 780 K corresponding to the stronger acid site, were observed on all the IM catalysts. With the increase of the $H_3PMo_{12}O_{40}$ loading, the intensity of the weaker acidity was enhanced, indicating that more $H_3PMo_{12}O_{40}$ was assembled with the increase of $H_3PMo_{12}O_{40}$ content.

Table 3. The effect of $H_3PMo_{12}O_{40}$ loading on methanol oxidation

$H_3PMo_{12}O_{40}$ (wt%)	Methanol conv. (%)	Selectivity (%)				
		HCHO	DME	MF	DMM	COx
9.1	17.79	16.76	14.73	12.88	53.80	1.83
13.2	22.41	12.18	32.81	13.76	39.57	1.68
16.6	25.53	18.39	31.31	18.80	29.29	2.21
20.9	37.80	15.63	36.79	20.60	25.00	2.94
28.5	47.55	14.17	47.81	22.88	11.79	3.35

$CH_3OH/O_2/Ar$=6.0/9.4/84.6, 453 K, 4,000 mL/g_{cat}·h

All these catalysts were tested and the results are shown in Table 3. As it could be seen that with the increase of $H_3PMo_{12}O_{40}$ loading, methanol conversion increased (from 17.79 to 47.55%) with DMM selectivity decreasing (from 53.80 to 11.79%), while DME selectivity concurrently increased. It appears that at lower $H_3PMo_{12}O_4$ loading, more protons were trapped through an $H_3PMo_{12}O_4$-support interaction and thus led to the decrease of acid sites, which was suitable for DMM synthesis. With the increase of $H_3PMo_{12}O_{40}$ loading, the Keggin clusters might behave similarly to bulk $H_3PMo_{12}O_4$ crystallites as verified by FT-IR spectra: acidic catalytic predominant suitable for DME formation [5,14]. This deduction was also verified by the FT-IR and NH_3-TPD results.

3. The Influence of Pretreatment Temperature

The influence of catalyst pretreatment temperature on methanol oxidation was also explored. Fig. 5 showed Raman spectra for $H_3PMo_{12}O_{40}$/SBA-15 (13.2 wt%) after exposure to ambient air at 298 K and after pretreatment in dry air at various temperatures. The Raman spectra of $H_3PMo_{12}O_{40}$ exposed to ambient air at 298 K was the same as that discussed in Fig. 2. With the pretreatment temperature increased from 298 K to 623 K, the characteristic peaks of H_3PMo_{12}

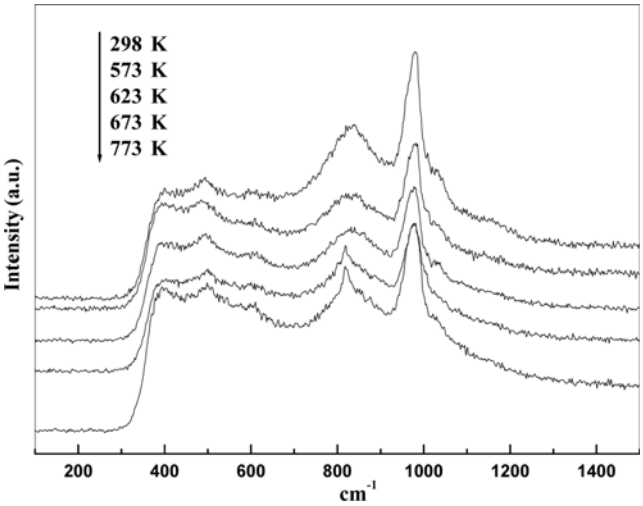

Fig. 5. The Raman spectra of the IM catalysts pretreated at different temperature.

O_{40} were always observed, only with a slight decrease of the intensity of the peak at 984 K which was sensitive to the dehydration process induced by the thermal treatment. With the temperature increased up to 673 K, the band at 1,012 cm^{-1} and 984 cm^{-1} was well remained, while a new band at 820 cm^{-1} corresponding to the characteristic peak of the β-MoO_3 appeared, indicating that the Keggin structure was partly decomposed into β-MoO_3 [5,15] and this trend continued up to 773 K. This phenomenon confirmed that the beginning transformation temperature from Keggin structure to MoO_3 was 673 K, which was higher than that of the bulk $H_3PMo_{12}O_{40}$ [15]. This result showed that the existence of SBA-15 could enhance the thermal stability of the $H_3PMo_{12}O_{40}$.

In order to measure the evolution of catalyst acidity, the NH_3-TPD profiles of the IM catalysts (13.2 wt%) pretreated at different temperature were recorded and the results were displayed in Fig. 6. As discussed above, two types of acid centers appeared: the weaker acid site associated with the constitutional protons and the stronger acid site assigned to the hydrated protons were observed on all the

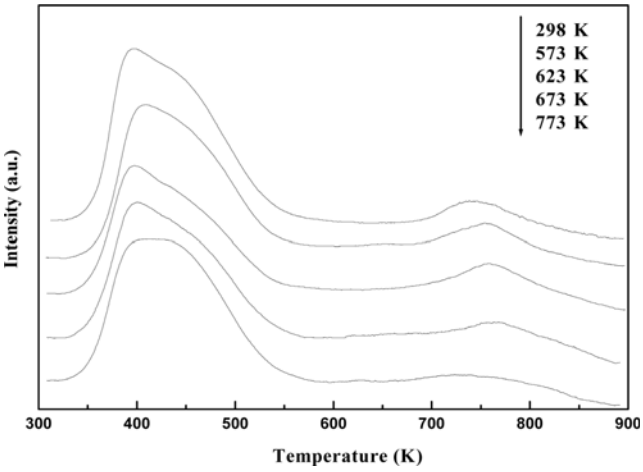

Fig. 6. The NH_3-TPD profiles of IM catalysts pretreated at different temperature.

Table 4. The effect of treatment temperature on methanol oxidation

Treatment temp. (K)	Methanol conv. (%)	Selectivity (%)				
		HCHO	DME	MF	DMM	COx
573	22.41	12.18	32.81	13.76	39.57	1.68
623	19.28	15.59	26.46	14.69	44.77	0.49
673	19.48	19.02	24.59	19.86	35.94	0.58
773	20.69	22.65	20.91	21.74	34.01	0.69

$H_3PMo_{12}O_{40}$/SBA-15 (13.2 wt%), $CH_3OH/O_2/Ar$=6.0/9.4/84.6, 453 K, 4,000 $mL/g_{cat}\cdot h$

catalysts [16]. With the temperature increased from 298 K to 623 K, the number of the weaker acid sites decreased with no much change of the stronger acid site. However, the number of the stronger acid sites declined to a large extent when the temperature increased up to 673 K, and this trend continued up to 773 K. The evolution of the acidity revealed the structure rearrangement of the Keggin structure. The decrease of the weaker acid site indicated the loss of some constitutional protons which was sensitive to thermal pretreatment without the degradation of the $H_3PMo_{12}O_{40}$ Keggin structure. While, the decrease of the stronger acid site showed the transformation from $H_3PMo_{12}O_{40}$ Keggin structure to MoO_3 [16], and this result was consistent with the Raman spectra.

The influence of thermal pretreatment on the performance of IM catalysts was investigated as shown in Table 4. Thermal pretreatment temperature showed remarkable influence on product selectivity. As the thermal pretreatment temperature increased, DMM selectivity underwent a peak value, DME selectivity decreased, HCHO and Methyl formate (MF) selectivity increased. However, the activity changed slightly (from 22.41 to 20.69%). The dehydroxylated Keggin structures of $H_3PMo_{12}O_{40}$ formed after pretreatment at 623 K appeared to provide an effective compromise between the redox sites required to form HCHO intermediates and the acid sites involved in acetalization HCHO-CH3OH reactions to form DMM. The partial decomposition of $H_3PMo_{12}O_{40}$ into crystalline β-MoO_3 reduced the number of acid sites as some of -OH groups were removed as H_2O, and thus the selectivity to DME declined. But the materials retained some of the redox properties typical of Mo oxides and formed HCHO and MF with high selectivity [5].

CONCLUSION

$H_3PMo_{12}O_{40}$ was more stable on the DS catalyst than on the IM catalyst due to the stronger chemical interaction between the host SBA-15 and the guest $H_3PMo_{12}O_{40}$ on DS catalyst. The partly decomposed $H_3PMo_{12}O_{40}$ on IM catalyst could provide proper acid sites for DMM synthesis. Moreover, SBA-15 support had stabilizing effect on $H_3PMo_{12}O_{40}$: the decomposition temperature of $H_3PMo_{12}O_{40}$ on SBA-15 was higher than that of bulk $H_3PMo_{12}O_{40}$. The increase of $H_3PMo_{12}O_{40}$ loading made the catalyst behave like the bulk $H_3PMo_{12}O_{40}$: more acidic preferring DME formation. In addition, the decrease in selectivity to DMM and DME observed for the $H_3PMo_{12}O_{40}$/SBA-15 catalysts with the increasing of pretreatment temperature was related to the decrease of the Bronsted acid centers of $H_3PMo_{12}O_{40}$ during its thermal transformation into β-MoO_3 phases.

ACKNOWLEDGMENT

This work was supported by the international Sci&Tech Cooperation Project of Ministry of Science and Technology of China (No. 2007DFC60110) and the Key Project of Natural Science Foundation of China (No. 20603045).

REFERENCES

1. G. P. Hagen and M. J. Spangler, US Patent, 6,265,528 (2001).
2. G. P. Hagen and M. J. Spangler, US Patent, 6,437,195 (2002).
3. Y. Yuan, H. Liu, H. Imoto, T. Shido and Y. Iwasawa, *J. Catal*., **51**, 195 (2000).
4. Y. Yuan, T. Shido and Y. Iwasawa, *J. Phys*. *Chem*. *B*, **106**, 2002 (4441).
5. H. C. Liu and E. S. Ilesia, *J. Phys. Chem*. *B*, **107**, 10840 (2007).
6. K. W. La, H. Kim, J. C. Jung, J. Lee, D. R. Park, S. H. Lee and I. K. Song, *Korean J. Chem. Eng*., **25**, 710 (2008).
7. L. M. Gomez Sainero, S. Damyanova and J. L. G. Fierro, *Appl. Catal. A*: *General*, **208**, 63 (2001).
8. I. V. Kozhevnikov, *Chem. Rev.*, **98**, 171 (1998).
9. N. Mizuno and M. Misono, *Chem. Rev.*, **98**, 198 (1998).
10. X. Yuan, J. Shen and G. li, *J. Catal.*, **23**, 9 (2002).
11. D. Zhao, J. Feng, M. Q. Huo, N. G. Fredrickson, H. Chmelka and B. F. Stuck, *Sci*., **279**, 548 (1998).
12. Z. Luan, M. Hartmann, D. Zhao and W. Zhou, *Chem. Mater*., **11**, 1621 (1999).
13. J. W. Lee, D. L. Cho, W. G. Shim and H. Moon, *Korean J. Chem. Eng*., **21**, 246 (2004).
14. C. R. Deltcheff, A. Aouissi, S. Launayb and M. Fournier, *J. Mole. Catal*. *A*: *Chemical*, **114**, 33 (1996).
15. C. R. Deltcheff, A. Aouissi, S. Launayb, M. M. Bettahar, S. Launay and M. Fournier, *J. Catal*., **164**, 16 (1996).
16. S. Damyanova, M. L. Cubeiro and J. L. G. Fierro, *J. Mole. Catal. A: Chemical*, **142**, 85 (1999).